Vacuum-ultraviolet stimulated emission from two-photon-excited molecular hydrogen

H. Pummer, H. Egger, T. S. Luk, T. Srinivasan, and C. K. Rhodes
Department of Physics, University of Illinois at Chicago, P. O. Box 4348, Chicago, Illinois 60680
(Received 21 March 1983)

Intense vacuum-ultraviolet stimulated emission in molecular hydrogen, on both the Lyman and Werner bands, following excitation by two-quantum absorption at 193 nm on the $X\,^1\Sigma_g^+ \rightarrow E,F\,^1\Sigma_g^+$ transition, has been observed. The shortest wavelength seen in the stimulated-emission spectrum was 117.6 nm corresponding to the $C\,^1\Pi_u \rightarrow X\,^1\Sigma_g^+$ (2-5) $Q(2)$ transition. The $C\,^1\Pi_u$ state appears to be populated with a mechanism involving electron collisions. The radiative cascade mechanism found to lead to the vacuum-ultraviolet emissions on the Lyman band also causes strong infrared stimulated emission to occur on the $E,F\,^1\Sigma_g^+ \rightarrow B\,^1\Sigma_u^+$ band. Two entirely separate radiative excitation channels are observed to play important roles in the state-selective molecular population of the $E,F\,^1\Sigma_g^+$ level. One involves two 193-nm quanta in the $X \leftarrow E,F$ amplitude while the other process combines a 193-nm quantum with a first Stokes-shifted photon in H_2. The optical Stark effect was seen to play a significant role in the excitation process with shifts of molecular resonances as large as $\sim 45\ cm^{-1}$. Substantial deviations from Born-Oppenheimer behavior, resulting in a dramatic shift of the stimulated spectrum depending upon the excited-state rotational quantum number, were clearly observed for molecular levels close to the potential maximum separating the inner and outer wells of the $E,F\,^1\Sigma_g^+$ state. The maximum energy observed in the strongest stimulated line was $\sim 100\ \mu J$, a value corresponding to an energy conversion efficiency of $\sim 0.5\%$. The pulse duration of the stimulated emission is estimated from collisional data to be ~ 10 ps, a figure indicating a maximum converted vacuum-ultraviolet power of ~ 10 MW.

I. INTRODUCTION

In the infrared spectral region, both parametric processes and direct multiphoton excitation[1] of excited states followed by down- or up-shifted laser emission[2] have been used extensively for the generation of coherent radiation in that range. With the development of tunable excimer lasers which can deliver narrow bandwidth[3-5] radiation in short,[6,7] high-intensity pulses of superior spatial quality, these techniques have also become attractive for the generation of high-power vacuum-ultraviolet (vuv) and extreme-ultraviolet (xuv) radiation.

Direct radiative excitation by multiquantum processes can be used to generate amplification in the vuv and xuv regions. Molecular hydrogen represents the essential paradigm of this basic mechanism in the vuv range on account of its fundamental nature and the presence of a known[8,9] two-quantum resonance on the $X\,^1\Sigma_g^+ \rightarrow E,F\,^1\Sigma_g^+$ transition at 193 nm. In this work the observation of efficient stimulated emission in the infrared on the $E,F\,^1\Sigma_g^+ \rightarrow B\,^1\Sigma_u^+$ band and vacuum ultraviolet on the Lyman and Werner bands[10] following two-photon excitation of the $E,F\,^1\Sigma_g^+$ state in H_2 using a 193-nm ArF* laser is described.

II. TWO-PHOTON TRANSITIONS IN H_2 AT 193 nm

The relevant potential energy curves in H_2 are illustrated[11] in Fig. 1. At 300 K the relative equilibrium rotational state populations in the ground $X\,^1\Sigma_g^+$ state for $J=0$, 1, 2, and 3 levels are 1.0, 4.9, 0.83, and 0.52, respectively. The lowest excited state that is optically connected to the ground state by a dipole transition is the $B\,^1\Sigma_u^+$ state, which has a radiative lifetime[12] of ~ 600 ps (the exact value depending upon the vibrational quantum number) and a collisional quenching rate[12] $k_B \sim 1.3 \times 10^{-9} cm^3/s$ at 300 K. As shown in Fig. 1, the first excited singlet gerade state $E,F\,^1\Sigma_g^+$ has a double minimum arising from the avoided crossing of the $E(1s\sigma 2s\sigma)$ and $F(2s\sigma)^2$ curves.[13] The radiative lifetime from this level has been determined, both experimentally[9] and theoretically,[13,14] to be ~ 90 ns with a corresponding collisional quenching rate that has been measured to be $k_E \sim 2.1 \times 10^{-9} cm^3/s$.

For the $X\,^1\Sigma_g^+ \rightarrow E,F\,^1\Sigma_g^+$ two-photon transition in H_2,

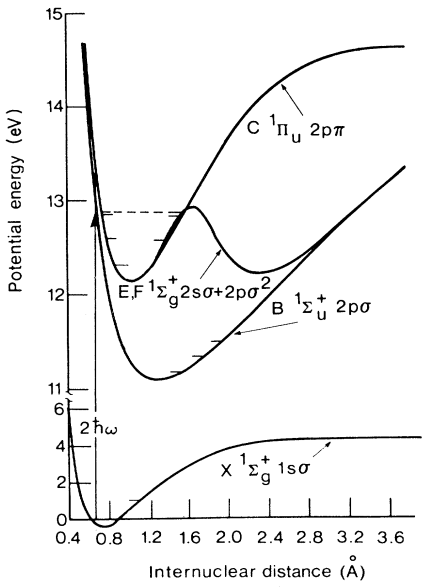

FIG. 1. Partial representation of potential-energy curves of H_2 (taken from Sharp, Ref. 11).

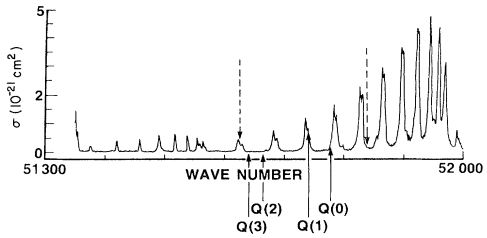

FIG. 2. Absorption cross section of O_2 in the range 51 300—52 000 cm^{-1}. The solid arrows indicate the transition frequencies of the Q branch of the $X\,^1\Sigma_g^+$ ($v=0$)-$E,F\,^1\Sigma_g^+$ ($v=2$) band. The broken arrows indicate the tuning range of the ArF* laser. Reprinted with permission from Pergamon Press (Ref. 18).

the Q-branch [$X(J)\rightarrow E,F(J)$] transitions are the strongest[15] for linearly polarized radiation. Given the available tuning range of the ArF* system in the vicinity of 193 nm, the transitions in H_2 that can be excited with two 193-nm quanta are the $Q(0)$, $Q(1)$, $Q(2)$, and $Q(3)$ transitions of the $X\,^1\Sigma_g^+\rightarrow E,F\,^1\Sigma_g^+$ (0-2) vibrational band.[15] Of particular interest are the $Q(2)$ and $Q(3)$ transitions which lie[16] at 103 328 cm^{-1} and 103 282 cm^{-1}, respectively, since they occur at frequencies for which interference from oxygen absorption at the corresponding 193-nm wavelengths is absent. Contrarily, Fig. 2 clearly shows that the frequency required for excitation of the $Q(1)$ transition (51 739.5 cm^{-1}) lies very close to the molecular Schumann-Runge[17,18] $R(19)$ line of the (4-0) band at 51 740 cm^{-1}. Similar interference from oxygen absorption also occurs for the 193-nm wavelength corresponding to the $Q(0)$ transition. Although these coincidences with oxygen lines appear to prevent the two-quantum excitation of the H_2 $Q(0)$ and $Q(1)$ transitions without the use of an oxygen-free path for the laser beam, the occurrence of the optical Stark effect, as discussed quantitatively below in Sec. IV A, obviates this limitation.

The two-photon coupling parameter, corresponding to the pump laser bandwidth of 5 cm^{-1} and a Doppler broadened H_2 linewidth has been estimated[8,9,19,20] to be

$$\alpha=2\times10^{-31}$$

(in cm^4/W). An important aspect to be noted from Fig. 1 is the near degeneracy between the $C\,^1\Pi_u^+$ state and the inner minimum of the $E,F\,^1\Sigma_g^+$ state. Since the $E(2s\sigma)$ and $C(2p\pi)$ states strongly resemble their atomic counterparts[13,21] at the relevant internuclear separation of ~1 Å, the two electronic states are connected by a large transition moment[22] with a magnitude of ~5 a.u. This causes the $C\,^1\Pi_u^+$ state to be the dominant intermediate state in the two-photon amplitude for excitation of the $E,F\,^1\Sigma_g^+$ from the $X\,^1\Sigma_g^+$ level, a conclusion first stated by Huo and Jaffe.[20]

As described below, a two-quantum coupling parameter of this magnitude and irradiation with 10-ps pulses enables approximately 1% of the H_2 ground-state population to be transferred to a rotationally specific excited state at an intensity of $\sim10^{11}$ W/cm^2 when proper account is made for losses due to photoionization of the $E,F\,^1\Sigma_g^+$ level at 193 nm. Therefore, at a medium density of 2×10^{19} cm^{-3}, with an allowance for rotational partition, inversion densities on the scale of $\sim10^{17}$ cm^{-3} can be generated. Since the optical cross sections for the inverted transitions are $\sim10^{-14}$ cm^2, a value leading to an optical gain constant of $\sim10^3$ cm^{-1}, strong stimulated emission is expected under these circumstances. Indeed, recent estimates by Huo and Jaffe[20] indicate that the coupling parameter α could be significantly larger than the earlier estimates leading to the value used above, a correction that would increase the gain constant by an appreciable factor.

It is known that molecular hydrogen is an efficient medium for stimulated Raman scattering of ultraviolet radiation.[23,24] Measurements with 10-ns ArF* laser pulses indicate that intense stimulated Raman scattering occurs in our apparatus at H_2 pressures $\gtrsim600$ Torr, and that $\sim25\%$ of the 193-nm fundamental wave is converted into the first-order Stokes line S_1 when the 193-nm beam is focused ($f/100$) into a cell containing ~1000 Torr of H_2. Therefore, in the high pressure regime (>600 Torr), two-quantum processes involving a Stokes shifted quantum could have an appreciable rate. Indeed, since the vibrational spacing[25] of the H_2 ground $X\,^1\Sigma_g^+$ state is almost exactly twice that characteristic of the excited $E,F\,^1\Sigma_g^+$ level, a two-quantum resonance occurs for the fundamental wave of 51 656 cm^{-1} with the corresponding Stokes S_1 at 47 501 cm^{-1} for the transition from $X\,^1\Sigma_g^+$ ($v=0$, $J=0$) to $E,F\,^1\Sigma_g^+$ ($v=0$, $J=0$). It will be seen that this Raman assisted channel is an important mode of molecular excitation.

III. EXPERIMENTAL APPARATUS

The 193-nm ArF* source[7] used in these experiments furnished an effective power of ~2 GW in a pulse duration of ~10 ps. This radiation had a measured bandwidth of ~5 cm^{-1} and a divergence of ~10 μrad, values close to their respective transform limits. The beam was focused with an $f=1.6$ m lens into the center of the experimental cell. The experimental cell consisted of a 2-m-long cell containing the hydrogen up to densities of ~2 amagat and was equipped with entrance and exit windows of CaF_2 and LiF, respectively. The pressure of H_2 inside the cell was determined by a standard baratron gauge. For observation of the vuv radiation, the LiF exit window of the cell was attached directly to the entrance slit of a 1-m vuv monochromator (McPherson 225) equipped with an optical multichannel analyzer (OMA PAR) at the exit slit to serve as the detector. The detection of infrared radiation with $\lambda\geq7000$ Å was accomplished similarly with the use of a suitable grating and a glass window at the entrance slit to eliminate all ultraviolet radiation.

IV. EXPERIMENTAL RESULTS

A. $B\,^1\Sigma_u^+\rightarrow X\,^1\Sigma_g^+$ emissions

Excitation of the hydrogen gas at frequencies corresponding to the two-quantum transitions discussed above leads to the observation of intense stimulated emission with a characteristic line structure. Tables I and II contain the identification[16] of the infrared and vuv transitions observed in the low pressure regime, 20—500 Torr, along with information on the observed intensities. The experi-

TABLE I. Transitions, corresponding wavelengths, and relative intensities of the observed stimulated emission in low-pressure (~ 20 Torr) H_2 on pumping the $Q(3)$ transition of the $X\,^1\Sigma_g^+ \rightarrow E,F\,^1\Sigma_g^+$ (0-2) band. Values in the third column are taken from the work of Dieke (Ref. 16).

Transition	Wavelength (Å) Present work	Previous work	Observed relative strength
Infrared			
$E \rightarrow B$			
2-2 $P(4)$	9222	9222.04	5
vuv			
$B \rightarrow X$			
2-8 $P(5)$	1531.5	1532.1	1
2-9 $R(3)$	1570.8	1571.4	5
2-9 $P(5)$	1584.9	1585.5	12
vuv			
$C \rightarrow X$			
2-5 $Q(3)$	1177.7	1178.3	<1

mentally observed wavelengths agree with the previous determined values,[10,16] within our experimental accuracy of ~ 20 cm^{-1}. This fact, concerning the wavelengths, will be considered further below in the discussion of the optical Stark effect.

With the ArF* laser tuned to the $Q(3)$ transition, stimulated emission on the lines shown in Fig. 3 was observed. The emission pattern displays the additional transitions illustrated in Fig. 4 for excitation corresponding to the $Q(2)$ transition. Two observations concerning the nature of

TABLE II. Transitions, corresponding wavelengths, and the relative intensities of the observed stimulated emission in low-pressure (20 Torr) H_2 on pumping the $Q(2)$ transition of the $X\,^1\Sigma_g^+ \rightarrow E,F\,^1\Sigma_g^+$ (0-2) band. Values in the third column are taken from the work of Dieke (Ref. 16).

Transition	Wavelength (Å) Present work	Previous work	Observed relative strength
Infrared			
$E \rightarrow B$			
2-1 $P(3)$	8370	8369.23	8
2-0 $P(3)$	7544.1	7544.06	0.8
vuv			
$B \rightarrow X$			
1-6 $P(4)$	1440.9	1440.7	3
1-6 $R(2)$	1428.8	1428.9	<1
1-7 $P(4)$	1499.6	1499.6	33
1-7 $R(2)$	1487.6	1487.7	13
1-8 $P(4)$	1557.4	1557.6	6
1-8 $R(2)$	1545.4	1545.7	1
vuv			
$C \rightarrow X$			
2-5 $Q(2)$	1176.3	1176.8	<1

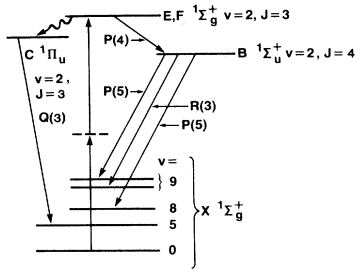

Wavelengths in nm:

E,F → B	B → X			C → X
2-2 P (4)	2-8 P(5)	2-9 P (5)	2-9 R (3)	2-5 Q (3)
922.2	153.2	158.5	157.1	117.8

FIG. 3. Stimulated emission from H_2 following $E,F \leftarrow X$ (2-0) $Q(3)$ two-photon excitation with 2 ArF* (193-nm) quanta. For the $E,F \rightarrow C$ transition, see text.

these stimulated spectra are noteworthy. The first involves the shift of the dominant $E,F \rightarrow B$ transition in the infrared from $(2 \rightarrow 2)$ $P(4)$ to $(2 \rightarrow 1)$ $P(3)$ upon changing from $Q(3)$ to $Q(2)$ excitation, an indication of a significant dependence of the wave function for nuclear coordinates on the rotational quantum number. The second point relates to the occurrence of stimulated emission stemming from the $J=3$ level (Fig. 3) with the 193-nm laser tuned to the frequency corresponding to the $Q(2)$ transition (Fig. 4). It is significant that the corresponding dual output did *not* occur under the excitation of the $Q(3)$ transition. No lines originating from the $J=2$ state due to the excitation of the $Q(2)$ transition have been observed with the laser tuned to the $Q(3)$ transition.

Qualitatively, the shift in the dominant infrared transition accompanying the change from $Q(3)$ to $Q(2)$ excitation can be explained by the fact that the inner-well $E\,^1\Sigma_g^+$ $(v=2,\ J=3)$ level is only a few hundred wave numbers ($\sim 200 \pm 150$ cm^{-1}) below the intermediate maximum of the E,F potential curve,[11] whereas the nearby $J=2$ level is

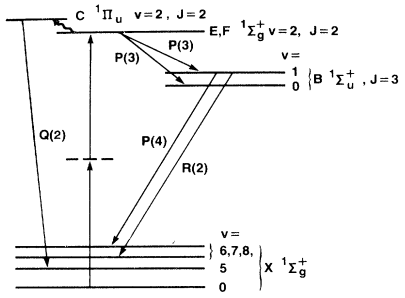

Wavelengths in nm:

E,F → B		C → X
2-1 P (3)	2-0 P (3)	2-5 Q (2)
836.9	754.4	117.6

B → X	1 - 6	1 - 7	1 - 8
P (4)	144.1	150.0	155.8
R (2)	142.9	148.8	154.6

FIG. 4. Stimulated emission from H_2 following $E,F \leftarrow X$ (2-0) $Q(2)$ two-photon excitation with 2 ArF* (193-nm) quanta. For the $E,F \rightarrow C$ transition, see text.

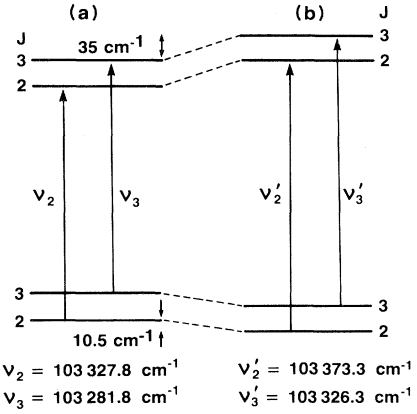

FIG. 5. Transition frequencies of $Q(2)$ and $Q(3)$ lines of $X\,^1\Sigma_g^+$ $(v=0)\rightarrow E,F\,^1\Sigma_g^+$ $(v=2)$ transition (a) in the absence and (b) in the presence of a strong optical field (shifts given for $I=6\times10^{11}$ W/cm^2).

lower by an additional 305 cm^{-1}. It has been established[26] theoretically that strong deviations from Born-Oppenheimer behavior occur for the $E,F\,^1\Sigma_g^+$ state, particularly in the region close to the maximum of the potential barrier and specific manifestations of this deviation have been recently observed by Marinero *et al.*[27] Therefore, due to the vibronic coupling between the inner and outer wells of this state and the consequently large deviation from Born-Oppenheimer behavior for the $(v=2, J=3)$ level of the E,F state, the (2-2) vibronic transition is preferred over the (2-1) transition predicted by Lin.[28] The peculiar nature of the $J=3$ level arising from its proximity to the potential maximum is also reflected in the anomalous spacings of the rotational levels. The energy difference between the $J=2$ and $J=3$ levels is 305 cm^{-1}, a value that stands in contrast to the 85 cm^{-1} difference separating the $J=1$ and $J=2$ states.[16]

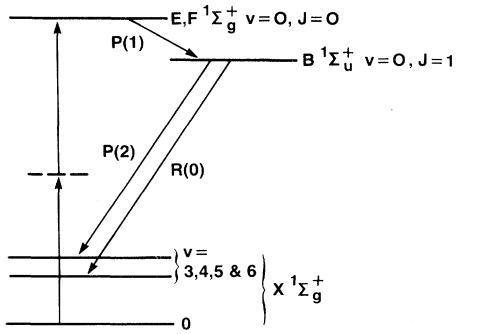

FIG. 6. Stimulated emission from H_2 following $E,F\leftarrow X$ (0-0) $Q(0)$ two-photon excitation with one fundamental and one Stokes-shifted ArF* photon.

The observation of stimulated emission originating from the $E,F\,^1\Sigma_g^+$ $(v=2, J=3)$ level upon excitation of the system at a frequency corresponding to the two-quantum $Q(2)$ transition, is direct evidence of the role of the optical Stark effect. Figure 5 illustrates the positions of the participating levels both in the presence and the absence of the 193-nm radiation field based upon previously performed estimates of the nonlinear coupling to this molecule.[29] As shown in Fig. 5, at an intensity of $\sim6\times10^{11}$ W/cm^2, the unshifted $Q(2)$ transition frequency becomes almost exactly equal to the radiatively shifted $Q(3)$ transition frequency. This condition can arise since the optical Stark effect is sufficient to *increase* the transition energy of the $Q(3)$ line by ~45 cm^{-1}, a value large in comparison to both the effective linewidth of the 193-nm radiation and the instrumental resolution used to register the stimulated transitions. Since strong two-photon excitation occurs in regions of the converging 193-nm beam in which the intensity spans the range of 10^{11} W/cm^2 to 10^{13} W/cm^2, the simultaneous excitation of the $Q(2)$ and $Q(3)$ transitions becomes possible, albeit in different spatial regions, and subsequent stimulated emission on both bands can arise. It is recalled that similar effects have been previously observed[30] for a two-photon—excited 16-μm laser in NH_3. It is important to note that, because of the sign of the radiative shift, the simultaneous excitation of the $Q(2)$ and $Q(3)$ transitions is not expected when the 193-nm laser wavelength is tuned to the $Q(3)$ line, a conclusion which is in agreement with experimental observations. Finally, we observe that optical Stark shifts on the scale observed (~45 cm^{-1}) are sufficient to shift the $Q(0)$ and $Q(1)$ transitions to frequencies for which no interfering oxygen absorption occurs (see Fig. 2), enabling those states to be excited as well.

At H_2 pressures above 600 Torr, an additional set of lines appears when the 193-nm excitation laser is tuned to the $E,F\leftarrow X$ (2-0) $(Q)(2)$ transition. These additional observed transitions are shown in Fig. 6 and Table III lists the pertinent data and identifications based on previous studies.[16] Inspection shows that the $E,F\leftarrow X$ (0-0) $Q(0)$

TABLE III. Transitions, corresponding wavelengths, and relative intensities of the observed stimulated emission in high-pressure (>600 Torr) H_2. Values in the third column are taken from the work of Dieke (Ref.16).

Transition	Wavelength (Å) Present work	Previous work	Observed relative strength
$E\rightarrow B$			
0-0 $P(1)$	11 210	11 159.1	
$B\rightarrow X$			
0-3 $R(0)$	1275.2	1274.6	<1
0-3 $P(2)$	1280	1279.5	<1
0-4 $R(0)$	1333.6	1333.5	6
0-4 $P(2)$	1339	1338.6	3
0-5 $R(0)$	1394.4	1393.7	21
0-5 $P(2)$	1399.8	1399	11
0-6 $R(0)$	1455.5	1454.9	2.5
0-6 $P(2)$	1460.9	1460.2	1

transition is only 16 cm^{-1} below the energy of one 193-nm fundamental plus one Stokes shifted ArF^* photon. As in the case discussed above, this transition energy is increased by 16 cm^{-1} by the optical Stark effect at an intensity of $\sim 2\times 10^{11}$ W/cm^2. As expected, no emission from the E,F ($v=0$) level is observed when the frequency of the 193-nm radiation is decreased by 22.5 cm^{-1} to the $E,F \leftarrow X$ (2-0) $Q(3)$ transition. Furthermore, the onset of these emissions agrees with the observed threshold for the production of stimulated first Stokes radiation in H_2, an experimental finding strongly reinforcing the conclusion concerning the role of the Raman shifted conversion.

B. $C\,^1\Pi_u \rightarrow X\,^1\Sigma_g^+$ emissions

In addition to the $B \rightarrow X$ emission lines discussed above, two strong stimulated lines, one at ~ 117.6 nm and the other at ~ 117.7 nm are observed upon exciting the $E,F\,^1\Sigma_g^+$ $v=2$, $J=2$ and $J=3$ levels, respectively. While the absolute instrumental wavelength calibration is accurate only to ~ 100 cm^{-1}, the spacing between the two lines has been determined to be 106 ± 7 cm^{-1}. Within the limits of experimental uncertainty, these two lines can be identified as the $Q(2)$ and $Q(3)$ transitions of the 2-5 Werner band. As shown in Fig. 4, for the $Q(2)$ line, the transfer of population from the $E,F\,^1\Sigma_g^+$ to the $C\,^1\Pi_u$ state requires an increase of 47 cm^{-1} in the molecular energy, a fact clearly ruling out the role of stimulated emission for this particular transition. The probable energy transfer mechanism is, however, the collision of the excited molecules with electrons produced by the photoionization of the $E,F\,^1\Sigma_g^+$ state. Since the $E(2s\sigma)$ and $C(2p\pi)$ states strongly resemble their atomic counterparts, the electron collisional rate constant can be estimated[31,32] to be $\sim 7\times 10^{-6}$ $cm^3\,s^{-1}$. Since electron densities of $\sim 10^{16}$ cm^{-3} are expected to be produced by photoionization, a collisional rate of transfer of $\sim 7\times 10^{10}$ s^{-1} is obtained, a value comparable to both the quenching rate of the E,F state by heavy-body collisions[8,9,12] and stimulated emission to the B state. A similar estimate for ion collisions indicates[31,32] that the corresponding ion rate is approximately one order of magnitude less than the electron rate. Detailed analysis of these collisional processes will be presented in a subsequent publication.

C. General properties of the stimulated transitions

All the lines in the infrared and vacuum ultraviolet classified as stimulated exhibited clear thresholds for emission and a spatial divergence matching that of the focused 193-nm excitation beam. Furthermore, since the stimulated transitions observed did *not* exhibit detectable optical Stark shifts with an instrumental resolution of ~ 15 cm^{-1}, although radiative shifts on the scale of ~ 45 cm^{-1} were observed in the process of two-quantum excitation, the experiments indicate that the time of the stimulated emission does not exactly coincide with that of the maximum intensity of 193-nm irradiation. Presumably, the stimulated output occurs at a time slightly later than that of peak excitation, since it is expected that the peak gain, proportional to the quotient of the population inversion and the linewidth, would be maximal at a point shortly after the peak excitation. Physically, the linewidth factor will provide the principal contribution, since appreciable broadening arising from the rate of photoionization will substantially reduce the gain for the range of intensities present at the peak of the 193-nm irradiation. Specifically, at an intensity of $\sim 10^{11}$ W/cm^2, the gain is depressed an order of magnitude by broadening from excited-state photoionization.[29]

Previous collisional studies[8,9,12] of the $E,F\,^1\Sigma_g^+$ and $B\,^1\Sigma_u^+$ states establish a lifetime of ~ 16 ps at a density of one amagat, a value indicating that the pulse width of the stimulated emission, at least in the higher-pressure range examined in these studies, is not appreciably greater than that time. Therefore, the combination of the radiative and collisional influences leads to an expected pulse length of ~ 10 ps for the stimulated output or, as discussed below, an output power of ~ 10 MW on the strongest vuv line. In this picture, since the transit time of the 193 nm excitation pulse through the physically active region is significantly greater than the 10-ps pulse width or the collisional lifetime at typical operating pressures, the radiating medium responds essentially as a traveling wave amplifier.

D. Efficiency of observed stimulated emission

A principal finding of these experimental studies is the observation of a conversion efficiency of 193-nm radiation to specific deep vuv lines approaching 1%. Since photoionization[9,19,33] and collisional losses[8,9] compete with the two-quantum mechanism for excitation, there exist fundamental relationships connecting the medium density, the vuv gain, the pulse width of the 193-nm excitation, and the conversion efficiency. We now estimate an upper bound for the efficiency expected under conditions comparable to those occurring in these studies.

For this estimate the overall conversion efficiency can be represented as a product of two factors. One factor describes the efficiency with which the incident 193-nm radiation is absorbed in the process of populating the upper level. The second factor takes into account the reduction in upper-state population due to photoionization and collisions. For a two-photon coupling parameter

$$\alpha = 2\times 10^{-31}$$

(in cm^4/W), based on the previously determined[9] values, the absorption efficiency is estimated to be $\sim 25\%$. In the above estimate, a 193-nm intensity of 5×10^{10} W/cm^2, an equilibrium population density of a ground-state rotational level $\sim 3\times 10^{18}$ cm^{-3}, and an active medium of length 10 cm have been assumed. Under these conditions, the fractional loss of E,F state population due to photoionization and collisional quenching can be calculated to be 80% for a photoionization cross section[9] of 2×10^{-18} cm^2 and a collisional rate constant[9] of 2.1×10^{-9} cm^3/s with an ultraviolet pulse duration of 10^{-11} s and a total medium density of 3×10^{19} cm^{-3}. Since a single stimulated line is generally much stronger than the others in our experiment (see Tables I and II), it will be assumed that the stimulated emission occurs on only one transition. Therefore, combining the absorption efficiency and radiation efficiency with the assumption that half of the inversion density can be extracted at $\lambda \sim 800$ nm under conditions of saturation, the resulting energy conversion efficiency for the infrared $E \rightarrow B$ transition is estimated to be 1.3%. Although the emitted quantum is significantly greater for the $B \rightarrow X$

transitions ($\lambda \sim 150$ nm), similar estimates for the $B \rightarrow X$ VUV band also indicate an energy conversion efficiency of $\sim 0.5\%$. In this latter case, additional losses arise from photoionization of the $B\,^1\Sigma_u^+$ state with a cross section that will be somewhat larger than that corresponding to the $E,F\,^1\Sigma_g^+$ level.[34] It should be noted, however, that the recent estimates of the two-photon $X \rightarrow E,F$ cross section performed by Huo and Jaffe[20] indicate a cross section larger by a factor of 6 than the one used in the appraisal of the efficiency made above. This suggests that, under optimum conditions, a maximum efficiency of $\sim 3\%$ could be achieved on the $B \rightarrow X$ band. In the present experiment, which does not correspond to the optimum conditions for efficient excitation, comparison with attenuated 193-nm radiation shows that the strongest transition B $(v=1, J=3) \rightarrow X$ $(v=7, J=4)$ (Table II) at $\lambda \sim 150$ nm contains an energy of ~ 100 μJ corresponding to an observed energy conversion efficiency of $\sim 0.5\%$.

V. CONCLUSIONS

Intense stimulated emission on the Werner and Lyman bands of H_2 is observed following two-photon excitation of the $X \rightarrow E,F$ transition with 193 nm, ~ 10 ps radiation. Stimulated emission on infrared transitions belonging to the $E,F \rightarrow B$ band is also observed. All the $B\,^1\Sigma_u^+ \rightarrow X\,^1\Sigma_g^+$ Lyman band stimulated lines can be attributed to direct radiative cascades originating from the state initially populated in the two-quantum excitation. For the $C\,^1\Pi_u \rightarrow X\,^1\Sigma_g^+$ Werner band, a mechanism involving electron collisions in energy transfer from the $E,F\,^1\Sigma_g^+$ state to the $C\,^1\Pi_u$ level is strongly implicated. Two different channels of excitation were found to populate the $E,F\,^1\Sigma_g^+$ levels, one involving two 193-nm quanta and the other combining a 193-nm quantum with a first Stokes-shifted photon. The optical Stark effect was seen to play a significant role in the excitation process with shifts of molecular resonances as large as ~ 45 cm^{-1}. In addition, a large deviation from Born-Oppenheimer behavior, resulting in an abrupt shift of the stimulated spectrum depending upon the excited-state rotational quantum number, was observed for molecular levels close to the potential maximum separating the inner and outer wells of the $E,F\,^1\Sigma_g^+$ state. The energy observed on the strongest line was ~ 100 μJ, a value corresponding to a conversion efficiency of $\sim 0.5\%$. The corresponding pulse duration has been estimated to be ~ 10 ps, a figure indicating a maximum converted vuv power of ~ 10 MW. Clearly, the general technique of nonlinear excitation studied in this work can be readily extended to a wide range of transitions in H_2, HD, and D_2 to provide a multitude of intense narrow bandwidth sources in the vacuum-ultraviolet region.

ACKNOWLEDGMENTS

The authors wish to acknowledge the expert technical assistance of M. J. Scaggs and J. R. Wright. We are grateful to K. Yoshino, O. E. Freeman, J. R. Esmond, and W. H. Parkinson and to Pergamon Press for making available and granting permission to reprint Fig. 2. This work was supported by the U.S. Office of Naval Research; the U.S. Air Force Office of Scientific Research under Grant No. AFOSR-79-0130, the National Science Foundation under Grant No. PHY-81-16626, and the Avionics Laboratory, Air Force Wright Aeronautical Laboratories, Wright Patterson U.S. Air Force Base, Ohio.

[1] *Topics in Applied Physics,* edited by Y.-R. Shen (Springer, New York, 1977).

[2] H. Pummer, W. K. Bischel, and C. K. Rhodes, J. Appl. Phys. 49, 976 (1978); D. Prosnitz, R. R. Jacobs, W. K. Bischel, and C. K. Rhodes, Appl. Phys. Lett. 32, 221 (1978); J. Eggleston, J. Dallarosa, W. K. Bischel, J. Bokor, and C. K. Rhodes, J. Appl. Phys. 50, 3867 (1979).

[3] R. T. Hawkins, H. Egger, J. Bokor, and C. K. Rhodes, Appl. Phys. Lett. 36, 391 (1980).

[4] J. C. White, J. Bokor, R. R. Freeman, and D. Henderson, Opt. Lett. 6, 293 (1981).

[5] H. Egger, T. Srinivasan, K. Hohla, H. Scheingraber, C. R. Vidal, H. Pummer, and C. K. Rhodes, Appl. Phys. Lett. 39, 37 (1981).

[6] P. H. Bucksbaum, J. Bokor, R. H. Storz, and J. C. White, Opt. Lett. 7, 399 (1982).

[7] H. Egger, T. S. Luk, K. Boyer, D. F. Muller, H. Pummer, T. Srinivasan, and C. K. Rhodes, Appl. Phys. Lett. 41, 1032 (1982).

[8] D. J. Kligler and C. K. Rhodes, Phys. Rev. Lett. 40, 309 (1978).

[9] D. J. Kligler, J. Bokor, and C. K. Rhodes, Phys. Rev. A 21, 607 (1980).

[10] R. W. Dreyfus and R. T. Hodgson, Phys. Rev. A 9, 2635 (1978); R. T. Hodgson and R. W. Dreyfus, Phys. Rev. Lett. 28, 536 (1972); H. Pummer, H. Egger, T. S. Luk, T. Srinivasan, and C. K. Rhodes, in *Proceedings of the Topical Meeting on Excimer Lasers,* Lake Tahoe, Nevada, 1983, edited by H. Egger, H. Pummer, and C. K. Rhodes (American Institute of Physics, New York, in press); T. Srinivasan, thesis, Department of Physics, University of Illinois at Chicago (unpublished).

[11] T. E. Sharp, Atomic Data 2, 119 (1971).

[12] H. Schmoranzer and J. Imschweiler, in *Proceedings of the Eighth International Conference on Atomic Physics, Göteborg, 1982,* Program and Abstracts, edited by I. Lindgren, A. Rosén, and S. Svanberg (Wallin and Dalholm Boktr. AB, Lund, 1982), p. A40.

[13] W. Kołos and L. Wolniewicz, J. Chem. Phys. 50, 3328 (1969).

[14] R. J. Spindler, J. Quant. Spectrosc. Radiat. Transfer 9, 1041 (1969).

[15] G. Herzberg, *Spectra of Diatomic Molecules* (Van Nostrand Reinhold, New York, 1950).

[16] G. H. Dieke, J. Mol. Spectrosc. 2, 494 (1958).

[17] M. Ackerman and F. Biaumé, J. Mol. Spectrosc. 35, 73 (1970).

[18] K. Yoshino, D. E. Freeman, J. R. Esmond, and W. H. Parkinson, Planet. Space. Sci. (in press).

[19] W. K. Bischel, J. Bokor, D. J. Kligler, and C. K. Rhodes, IEEE J. Quantum Electron. QE-15, 380 (1979).

[20] W. M. Huo and R. L. Jaffe, private communications.

[21] W. Kołos and L. Wolniewicz, J. Chem. Phys. 43, 2429 (1965).

[22] H. A. Bethe and E. E. Salpeter, *Quantum Mechanics of One- and Two-Electron Atoms* (Plenum, New York, 1977).

[23] T. R. Loree, R. C. Sze, and D. L. Baker, Appl. Phys. Lett. 31, 37 (1977).

[24] R. S. Hargrove and J. A. Paisner, in *Proceedings of the Topical*

Meeting on Excimer Lasers, Charleston, South Carolina 1979 (Optical Society of America, Washington, DC, 1979), p. ThA-6.

[25]K. P. Huber and G. Herzberg, *Molecular Spectra and Molecular Structure, IV: Constant of Diatomic Molecules* (Van Nostrand Reinhold, New York, 1979).

[26]L. Wolniewicz and K. Dressler, J. Mol. Spectrosc. 67, 416 (1977).

[27]E. E. Marinero, C. T. Rettner, and R. N. Zare, private communication.

[28]C. S. Lin, J. Chem. Phys. 60, 4660 (1974).

[29]T. Srinivasan, H. Egger, H. Pummer, and C. K. Rhodes, IEEE J. Quantum Electron (in press); P. Avon, C. Cohen-Tannoudji, J. Dupont-Roc, and C. Fabre, J. Phys. (Paris) 9, 993 (1976).

[30]H. Pummer, W. K. Bischel, and C. K. Rhodes, J. Appl. Phys. 49, 976 (1978); J. Bokor, W. K. Bischel, and C. K. Rhodes, J. Appl. Phys. 50, 4541 (1979).

[31]L. Spitzer and J. L. Greenstein, Astrophys. J. 114, 407 (1951).

[32]E. M. Purcell, Astrophys. J. 116, 457 (1952).

[33]J. Bokor, J. Zavelovich, and C. K. Rhodes, Phys. Rev. A 21, 1453 (1980).

[34]A. Cohn, J. Chem. Phys. 57, 2456 (1972).